Global Journal of Engineering Science and Research Management

STUDY OF THE OPTICAL CHARACTERISTICS OF EPITAXIAL $PbS_{1-y}Se_y$ LAYERS

A.M. Pashaev1, O.I. Davarashvili2, M. I. Enukashvili2, Z. G.Akhvlediani2,3, L.P.Bychkova2, V.P. Zlomanov4

*1National Aviation Academy, Baku A2-1045, Azerbaijan.
2Iv. Javakhishvili Tbilisi State University, Tbilisi 0128, Georgia.
3E.Andronikashvili Institute of Physics, Tbilisi 0186, Georgia.
5M.Lomonosov Moscow State University, Moscow 119899, Russia.

ABSTRACT

For designing new high-performance IR optoelectronic devices based on the strained layers of semiconductors $PbS_{1-y}Se_y$, the methods of determination of the optical characteristics of particular compositions at the concentration of currentcarriers$\leq 10^{18} cm^{-3}$ were improved. When studying the dispersion of the refractive index in the layers more than 4 μm in thickness, it was found that, under these conditions, the refractive index in a wider-band layer was higher than in a narrow-band layer at the concentration of current carriers $\sim 10^{19} cm^{-3}$. The deviation from linearity at long wavelengths associated with plasma absorption. In the long-wave region, the additional absorption in the layers of this typeis revealed at a lower level than in thinner ones and can be explained by the absorption at the layer-substrate interface reduced to the entire thickness or by transitions between different branches of the allowed band in a particular case at a low concentration of current carriers in these layers.

INTRODUCTION

From IV-VI semiconductors, solid solutions $Pb_{1-x}Sn_xTe$ and $PbS_{1-y}Se_y$have found the most application. At the same time, unlike $Pb_{1-x}Sn_xTe$, when the energy range 0.32 - 0 eV is overlapped because of band inversion (300 K), a narrower energy range 0.29-0.41 eV is overlapped for solid solutions$PbS_{1-y}Se_y$. While at 300 K this corresponds to the wavelength range 3-4.3 nm, at 77 K this range extends to 7μm. Therefore, the radiation sources and detectors based on these solid solutions are used for gas analysis: CO, CO_2, SO_2, NO, NO_2, CH_4, etc. [1]. For cosmic and terrestrial IR probing, we suggest designing the high-sensitivity high-temperature IR photodetectors based on strained layers doped with variable-valence impurities Cr or In and grown on dielectric substrates with specified mismatch [2]. As the studies on strained layers PbSe showed [3], to accomplish this task, it is necessary to know the optical parameters of semiconductors. In the case of solid solutions, it concerns particular compositions, because the arrangement of impurity levels in the forbidden gap depends on the composition and temperature in order to achieve the outmost compensation of electrically active nonstoichiometric defects and impuritiesthemselves,and the realization of a quasidielectric state.

The application of strained layers of solid solutions $PbS_{1-y}Se_y$ will allow subsequently finding the optimal compositions for arrangement of impurity levels deep in the forbidden gap and determining the reliability of devices based on thin layers.

This work deals with the investigation of optical characteristics of different compositions of layers $PbS_{1-y}Se_y$.

OBJECTS AND METHODS OF INVESTIGATION

The objects of investigation were epitaxial layers $PbS_{1-y}Se_y$ grown on cubic crystals CaF_2(a=5.462Å) and BaF_2(a=6.200Å) having the coefficients of thermal expansion close to those of the semiconductors under study. The epitaxial layers $PbS_{1-y}Se_y$ were grown by molecular epitaxy with "a hot wall" [4].
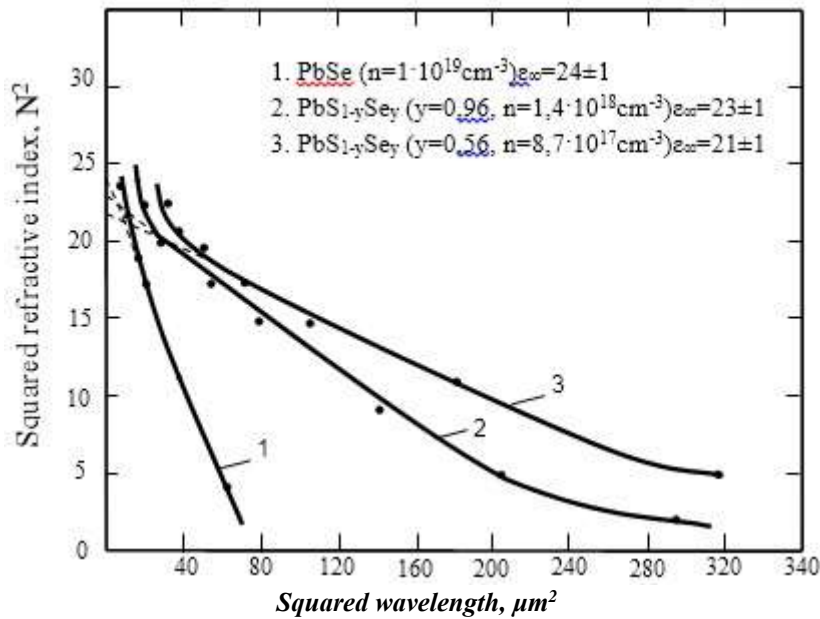
Fig. 1. Dispersion dependence of the squared refractive index on the squared wavelength for the $PbS_{1-y}Se_y$ (y=0.96)

The temperature of the epitaxy source, polycrystalline PbSSe of the composition corresponding to that of the layer (due to the congruence of evaporation of IV-VI semiconductors), was equal to 540-570°C, while the temperature of substrates CaF_2 and BaF_2 was within the range of 320-350°C.

Table 1. Data on the refractive indices and reflection coefficients for the $PbS_{1-y}Se_y$ layers(y=0.96, d=5.8 μm)

λ, μm	hv,eV	N(PbSSe)	N(CaF$_2$)	r_1	r_2	Texp.
17,24	0,072	1,486	1,240	0,196	0,090	0,400
14,29	0,087	2,463	1,280	0,422	0,316	0,420
11,90	0,104	3,079	1,320	0,510	0,400	0,420
10,10	0,123	3,483	1,330	0,554	0,447	0,400
8,80	0,141	3,794	1,370	0,583	0,469	0,410
7,75	0,160	4,010	1,380	0,601	0,488	0,400
6,92	0,179	4,176	1,385	0,614	0,502	0,400
6,25	0,198	4,310	1,390	0,623	0,512	0,400
5,81	0,213	4,511	1,400	0,637	0,526	0,400
5,32	0,233	4,585	1,400	0,642	0,532	0,400
4,95	0,250	4,694	1,410	0,649	0,538	0,370
4,63	0,268	4,789	1,410	0,655	0,545	0,320
4,44	0,279	4,837	1,414	0,657	0,548	0,160
4,29	0,289	4,884	1,418	0,660	0,550	0,150
4,15	0,299	4,931	1,422	0,663	0,552	0,135
4,02	0,309	4,978	1,426	0,665	0,555	0,065
3,89	0,319	5,025	1,429	0,668	0,557	0,052

For controlling the concentration of current carriers in the layers over the range from $5 \cdot 10^{17}$ to $5 \cdot 10^{18}$ cm^{-3}, the temperature of an additional source of Se was varied from 110°C to 130°C, while the molecular composition of the solid solution hardly changed. The growth rate of layers was varied by varying the temperature of the epitaxy source and the distance between the open end of the quartz ampoule with that source and the substrate from 1 to 3 mm, the growth rate making up 0.1-2.0 nm/s.

Two layers were selected for the investigation: the first one was grown on the CaF$_2$ substrate, it was 5.8 µm thick, and had the lattice constant equal to a=6.118 Å and the composition y=0.96. The second layer was grown on the BaF$_2$ substrate, it was4,1µm thick, and had the lattice constant equal to a=6.044 Å and the composition y=0.56.

The concentration of current carriers in the first layer made up $1.4 \cdot 10^{18}$ cm^{-3}, in the second layer it was a little lower and was equal to $8.7 \cdot 10^{17}$ cm^{-3}. The thickness and the lattice constants (by which the composition was determined) were studied by the method of X-ray diffraction using the Co$_{k_\alpha}$ radiation and reflections from crystallographic planes (333) and (444) [5].

Table 2. Data on the absorption coefficients and their squares for the PbS$_{1-y}$Se$_y$ layers(y=0.96, d=5.8µm)

hv, eV	α,cm^{-1}	$\alpha_{fr.car}$,cm^{-1}	$\alpha^* = \alpha - \alpha_{fr.car}$, cm^{-1}	$(\alpha^*)^2$, cm^{-2}	$(\alpha^* hv)^2$, cm^{-2}eV^2
0,072	1539	1524	15	7,19E-03	3,72E-05
0,087	1211	631	580	3,36E+05	2,53E+03
0,104	1076	351	725	5,25E+05	5,70E+03
0,123	1059	223	836	6,99E+05	1,05E+04
0,141	975	156	819	6,71E+05	1,33E+04
0,160	969	114	855	7,31E+05	1,87E+04
0,179	942	87	855	7,31E+05	2,35E+04
0,198	921	69	852	7,26E+05	2,86E+04
0,213	892	57	835	6,97E+05	3,17E+04
0,233	881	47	834	6,95E+05	3,78E+04
0,250	955	40	915	8,38E+05	5,26E+04
0,268	1055	34	1021	1,04E+06	7,47E+04
0,279	1113	31	1081	1,17E+06	9,10E+04
0,289	1775	29	1746	3,05E+06	2,54E+05
0,299	1895	27	1869	3,49E+06	3,12E+05
0,309	2900	25	2875	8,27E+06	7,88E+05
0,319	3611	23	3588	1,29E+07	1,31E+06

The concentration and mobility of current carriers were studied by a four-probe method. The optical characteristics of epitaxial layers were determined by analyzing the transmission spectra recorded at 300 K by using the two-beam prism-diffraction spectrophotometer SPECORD-75IR. Masks and diaphragms were used for calibration of the transmission scale [6].

RESULTS AND DISCUSSION

In the transmission spectra of the epitaxial layer 5.8 µm thick, we recorded 12 interference maxima, which is almost twice as much as in the layers 1.8 µm thick. Such a result is associated with the fact that, at this thickness, according to the dependence 2Nd=$m\lambda$ (1), there belong a greater number of half-waves with their overlapping in the phase and formation of interference extrema. Having determined the order of interference, we represent the diffraction dependence N^2=$f(\lambda^2)$ in Fig. 1. According to the well-known theoretical wavelength dependence of dielectric constant [7], it is linear in its large portion.
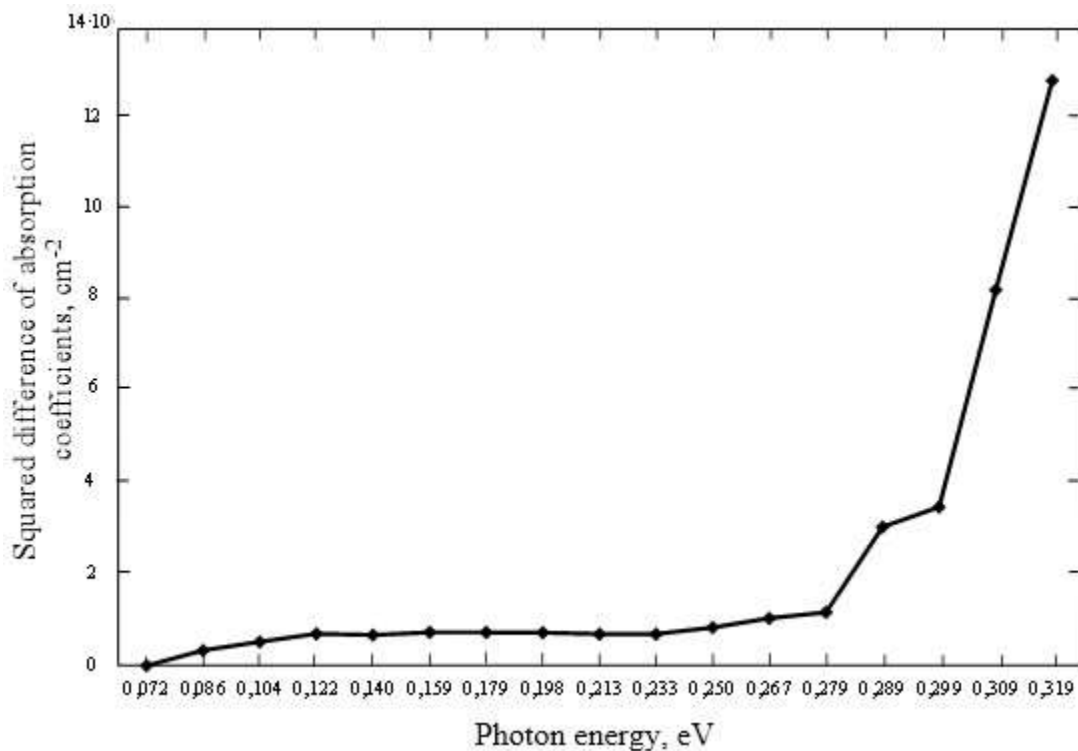
Fig. 2.Photon energy dependence of the squared difference of absorption coefficients for the PbS$_{1-y}$Se$_y$ layer (y=0.96)

Deviation from the linearity at long wavelengths is associated with the approximation of the refractive index to one when the incident radiation approximates the plasma frequency, while the reflection coefficient approximates zero. Extrapolation of this dependence to the zero wavelength leads to $\varepsilon_\infty= 23\pm1$.According to the theory, a jump in the refractive index (associated with a rapid increase in the absorption coefficient at the fundamental absorption edge) was naturally revealed in the vicinity of the forbidden gap width, and, as is evident from the hereinafter, it was equal to $\lambda^2=18.5\mu m^2$. For comparison, in Fig. 1 is also shown the dispersion dependence of the refractive index of the epitaxial PbSe layer 1.8 μm thick [8]. At a higher concentration of current carriers in the PbSe layer equal to ~10^{19} cm^{-3}, this dependence is located lower than for the PbS$_{1-y}$Se$_y$ layer with somewhat larger forbidden gap width.
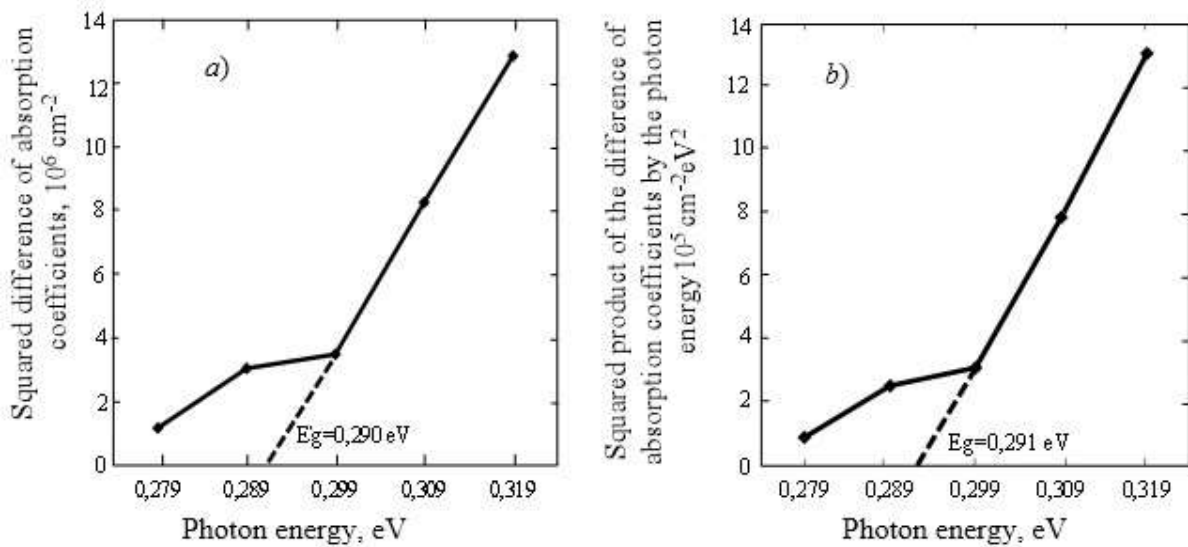
It should be emphasized that the dispersion dependences of the refractive index along with deformation potentials allowus to determine corrections for the refractive index in strained layers.

Like our previous work[9], the analysis of optical transmission spectra was performed by the model of Fabry-Perot interferometer , which was useful in this case too because of uniform layers and a parallel layer surface and a growth plane on, the substrate CaF$_2$. According to the model, the structure PbS$_{1-y}$Se$_y$/CaF$_2$ is considered as a resonator where the transmission T is determined as:

$$T=(1- r_1)^2(1- r_2)^2\exp(2\beta_i d)/[(1- R)^2+4R\sin^2(\beta d)] \qquad (2)$$

where $r_1=(N_l-N_{air})/(N_l+ N_{air})$ is the reflection coefficient by the amplitude at the layer-air interface,$r_2=(N_l-N_{sub})/(N_l+ N_{sub})$ is the reflection coefficient by the amplitude at the layer-substrate interface,N_l, N_{air} and $N_{sub}$are the refractive indices of the layer, air and the substrate, respectively; $R= r_1r_2\exp(\beta_i d)$ is the reflection coefficient by power, $\beta=2\pi N/\lambda$, $\beta_i= - \alpha/2$, α is the absorption coefficient by the spectrum. Assuming y= $\exp(2\beta_i d)= \exp(-\alpha d)$, we get the equation for determination of y :

$$T(r_1r_2)^2 y^2 - [(1- r_1^2)(1- r_2^2) + Tr_1r_2 - 4\ Tr_1r_2\sin^2(2\pi Nd)/\lambda]y + T=0 \qquad (3)$$

Fig.3a,b. Photon energy and the corresponding values of the squared difference of absorption coefficients (a) and of the squared product of the difference of absorption coefficients by the photon energy (b) for the PbS$_{1-y}$Se$_y$ layer (y=0.96)

Certain values of the refractive indices and reflection coefficients of epitaxial layers PbS$_{1-y}$Se$_y$ by thespectrum are given in Table 1. In Table 1 are also given the corresponding values of the refractive index of the CaF$_2$ substrate and the values of transmission averagedbetween the interference maxima and minima by the spectrum. There are also given the data by 5 extrapolated points in the short wavelength region.

Table 3. Data on the refractive indices for thePbS$_{1-y}$Se$_y$ layers (y=0.56, d=4,1μm)

№	1	2	3	4	5	6	7	8	9	10	11
λ	3.73	4.03	4.39	4.83	5.41	6.15	7.14	8.47	10.42	13.51	17.86
N	5.20	5.04	4.93	4.83	4.73	4.62	4.46	4.24	3.91	3.38	2.23

Neglecting the absorption in the layer,it is possible to compare the calculated and experimental values of transmission and to ascertain that all the maxima are real.

The values of the absorption coefficient calculated by Eq(3) showed the maximum which is likely related topreferential absorption by current carriers at long wavelengths and band-band absorption at short wavelengths.

Table 4. Data on the reflection and absorption coefficients for the PbS$_{1-y}$Se$_y$ layers (y=0.56, d=4,1 μm)

#	λ,μm	N(PbS$_{1-y}$Se$_y$)	r$_1$	r$_2$	T$_{exp.}$	hv, eV	α,cm^{-1}	α^{*2}=(α- α$_{fr.car.}$)^2, cm^{-2}	(α*hv)^2,cm^{-2}eV^2
1	3.85	5.18	0.6761	0.5570	0.230	0.322	1184	1.32E+06	1.38E+05
2	3.73	5.20	0.6774	0.5586	0.250	0.332	1553	2.32E+06	2.56E+05
3	3.58	5.20	0.6775	0.5587	0.135	0.346	2536	6.32E+06	7.49E+05
4	3.55	5.21	0.6776	0.5588	0.120	0.350	2759	7.46E+06	9.12E+05
5	3.51	5.21	0.6779	0.5592	0.117	0.353	3228	1.02E+07	1.28E+06
6	3.46	5.22	0.6781	0.5602	0.105	0.358	3602	1.28E+07	1.64E+06
7	3.42	5.22	0.6784	0.5605	0.077	0.363	3971	1.56E+07	2.05E+06
8	3.33	5.21	0.6779	0.5598	0.059	0.372	4263	1.80E+07	2.49E+06

9	3.28	5.22		0.6781	0.5602	0.055	0.378	4716	2.20E+07	3.15E+06

To determine the forbidden gap width by straightening the squared absorption coefficients associated with the band-band transitions, we should subtract the absorption by free carriers

$$\alpha_{fr.car.} = e^3 n \lambda^p / \pi^2 \mu N m^2 \qquad (4)$$

(where n is the concentration of current carriers, N is the refractive index, μ and m are the mobility and the effective mass of current carriers, respectively) from the total absorption. The quantity p varies from 1.5 to 2 with scattering by acoustic lattice oscillations and depending on the concentration of current carriers, and it increases in these limits with an increase in the concentration of current carriers from the level of 10^{18} and higher. At $p=2$, m=0.08m$_0$ and μ=1080 cm^2/V·s, the values of absorption by free carriers by the spectrum were calculated. The calculated data on $(\alpha - \alpha_{fr.car.})$,$(\alpha - \alpha_{fr.car.})^2$ and$[(\alpha - \alpha_{fr.car.})h\nu]^2$ as a function of hν are given in Table 2.

In Fig. 2 is shown the dependence $(\alpha - \alpha_{fr.car.})^2 = f(h\nu)$. From Table 2 and Fig. 2 it is evident that the values of α and $\alpha_{fr.car.}$are similar at 0.072eV (17.24μm), but in the general case they do not coincide and are determined separately.

It is noteworthy that, between the long wavelength absorption by free carriers and the incipient band-band absorption, additional absorption was detected at the level of 600-800 cm^{-1}. If we model equate the absorption by free carriers to the total absorption by the spectrum, the transmission would be equal to 0.85-0.95, which differs significantly from the experimental value. In this case smaller values of the additional absorption in comparison with the thinner layer can be referred to the absorption associated with the states at the layer-substrate interface and redistributed in the entire thickness of the layer at the same time. The presence of a maximum in such dependence does not exclude the contribution of possible transitions between different branches of the allowed band [10].
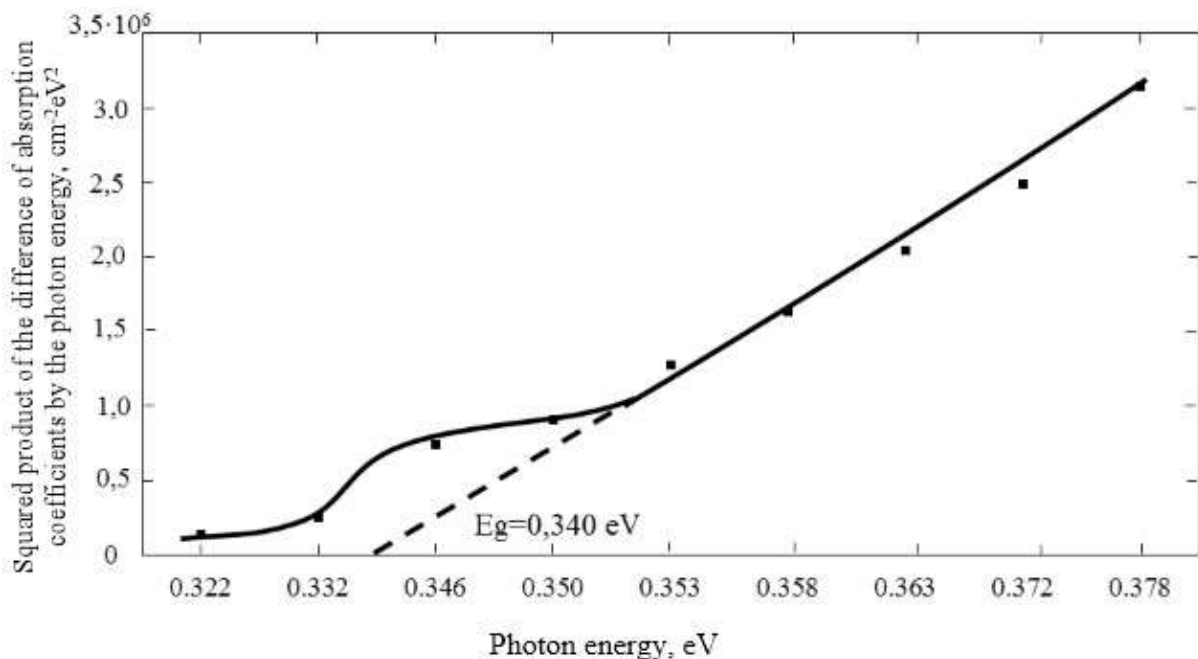

Fig. 4.Photon energydependence of the squared product of the difference of absorption coefficients by the photon energy for the PbS$_{1-y}$Se$_y$ layer (y=0.56)

In Fig. 3a,b are shown the dependences for two types of straightening $(\alpha - \alpha_{fr.car.})^2 = f(h\nu)$ and$[(\alpha - \alpha_{fr.car.})h\nu]^2 = f(h\nu)$ in the narrow wavelength range. Their straightening gives close values: E$_g$=0.291 eV, which corresponds to the composition y=0.96. Close values of E$_g$in both cases is associated with a slight shift of hν in the straightening region, but mostly with the absence of degeneration at this concentration of current carriers in the layer. It should be noted that, when the refractive indices vary by 10 %, the values of E$_g$ hardly change.

Global Journal of Engineering Science and Research Management

Based on the analysis performed, the most important for determination of the forbidden gap width is the study of the straightening of squared absorption coefficients in the narrow wavelength range.

Table 3 gives the data on the indices of refraction in the entire spectral range for the layer 4,1μmthick, and the corresponding dispersion dependence is shown in Fig. 1. Due to a lower concentration of current carriers in this layer, the dispersion dependence lies higher than the preceding ones, but $\varepsilon_\infty=21\pm1$. In this case, at long wavelengths, a deviation from the linear dependence $N^2=f(\lambda^2)$ is also observed. At the same time, the refractive index does not approximate one due to the decrease in the plasma frequency with the increasing effective mass of current carriers and their lower concentration in the layer at higher content of PbS.

In Table 4 are given the data on the refractive indices, reflection coefficients r_1 and r_2, transmission, and corresponding absorption coefficients. In Fig. 4 is shown the dependence $[(\alpha - \alpha_{fr.car.})h\nu]^2=f(h\nu)$ for this layer. Straightening of the squared product of absorption coefficients by the photon energy yielded $E_g=0.340eV$, which corresponds to the layer composition y=0.56 determined according to the linear dependence of the forbidden gap width on the composition of solid solutionsPbS$_{1-y}$Se$_y$ [11]. It is noteworthy that the squares of wavelengths of both layers under study equal to 18.5 and 12.9 μm^2 correspond to their forbidden gap width and jump region$\Delta\varepsilon$(Fig. 1), as it follows from the theory.

CONCLUSIONS

In this work we improved the methods of determination of optical characteristics such as the index of refraction N, the reflection coefficient r, the absorption coefficient α, the high-frequency dielectric constant ε_∞ and the forbidden gap width E_g for different compositions of solid solutions PbS$_{1-y}$Se$_y$. The high-frequency dielectric constant calculated by dispersion dependences varies with the composition of solid solutions. The deviation from the linear dispersion dependence at long wavelengths occurs because of the approximation to the plasma frequency. It was revealed that, in thicker layers, the additional absorption manifests itself at a lower level than in thin ones, and it could be associated with the absorption redistributed in the entire thickness of the layer at the layer-substrate interfaceor by transitions between different branches of the allowed band in a particular case at a low concentration of current carriers in these layers. The quantity E_g varies linearly depending on the composition of the solid solution at the concentration of current carriers $\leq 10^{18}$ cm^{-3}.

REFERENCES

1. A.M. Pashaev, O.I. Davarashvili, M.I. Enukashvili, Z.G. Akhvlediani, L.P. Bychkova , V. P. Zlomanov. Solid solutions of IV-VI semiconductors with substitution in the anion sublattice. Bulletin of the Georgian National Academy of Sciences, 2014, 40, 2-3, 4-10.
2. A.M. Pashaev, O.I. Davarashvili, V. A. Aliyev, M.I. Enukashvili, V. P. Zlomanov. Regular connection between the simultaneous stabilization of the Fermi level and transformation of the elastic properties of narrow-band IV-VI semiconductors, and their corversion into the dielectric state . Scientific discovery, Certificate No 340, In Collection of Scientific Discoveries and Hypotheses. International Academy of Scientific Discoveries, Moscow, 2008.
3. A.Pashaev, O.Davarashvili, Z.Akhvlediani,M.Enukashvili, R. Gulyaev,V. Zlomanov . Unrelaxed state in epitaxial heterostructures based on lead selenide . Journal of Modern Physics, 2012, 3, 6, 502-510.
4. A.M. Pashaev, O.I. Davarashvili, Z.G. Akhvlediani,M.I. Enukashvili, R. G. Gulyaev ,L.P. Bychkova . Epitaxial lead selenide layers over a wide range of their thickness on dielectric substrates . Journal of MaterialsScience and Engineering, 2013, B 3(2), 97-103.
5. A.M. Pashaev, O.I. Davarashvili,M.I. Enukashvili, L. P. Bychkova, R. G. Gulyaev, M A. Dzagania ,V. P. Zlomanov.The lattice constant as an indicator of the technology and properties of IV-VI semiconductors .Bulletin of the Georgian National Academy of Sciences, 2014, 40, 2-3,11-17.
6. A.M. Pashaev, O.I. Davarashvili, Z.G. Akhvlediani,M.I. Enukashvili, L.P. Bychkova, M. A. Dzagania . Study of the forbidden gap width of strained epitaxial lead selenidelayers . Journal of Materials Science and Engineering , 2012, 2, 2, 142-150.
7. Y. I. Ravich, B. A. Efimova ,I. A. Smirnov . The methods of investigation of semiconductors applied to lead chalcogenidesPbTe, PbSe and PbS .Nauka, Moscow, 1968.
8. A.M. Pashaev, O.I. Davarashvili, M.I. Enukashvili, L.P. Bychkova and V. P. Zlomanov. Analysis of the optical transmission spectra of epitaxial lead selenidelayers . Transactions of NAS of Azerbaijan .2011, 13, 3, 3-12.

Global Journal of Engineering Science and Research Management

9. A.M. Pashaev, O.I. Davarashvili, M.I. Enukashvili, Z.G. Akhvlediani, L.P. Bychkova,M. A. Dzagania .Successive approximations in the analysis of the optical transmission spectra of leadselenidenanolayers . Bulletin of the Georgian National Academy of Sciences, 2012, 38,2-3,186-192.
10. A.M. Pashaev, O.I. Davarashvili, M.I. Enukashvili, Z.G. Akhvlediani, L.P. Bychkova, M. A. Dzagania, V. P. Zlomanov . Analysis of the absorption spectra of epitaxial lead telluride and lead selenidelayers . IJEIT, 2015, vol. 4, issue 11, 193-198.
11. A.M. Pashaev, O.I. Davarashvili, M.I. Enukashvili, Z.G. Akhvlediani, L.P. Bychkova , V. P. Zlomanov . Control of the forbidden gap width by varying the composition and the thickness of the layers of IV-VI semiconductors .NanoStudies, 2015, 12, 5-10.